ELSEVIER

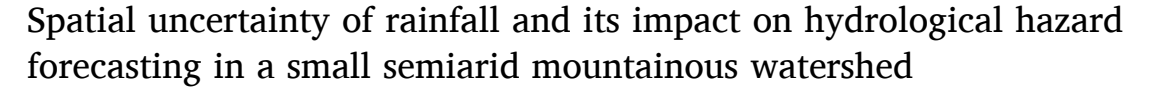
Contents lists available at ScienceDirect

Journal of Hydrology

journal homepage: www.elsevier.com/locate/jhydrol



Research papers



Guo Xiaojun a,b,* , Cui Peng a,b , Chen Xingchang c , Li Yong a , Zhang Ju c , Sun Yuqing c

- a Key Laboratory of Mountain Hazards and Surface Process/Institute of Mountain Hazards and Environment, Chinese Academy of Sciences, Chengdu 610041, China
- ^b CAS Center for Excellence in Tibetan Plateau Earth Sciences, Beijing 100101, China
- ^c School of Environment and Resource, Southwest University of Science and Technology, Mianyang 621020, China

ARTICLE INFO

This manuscript was handled by Marco Borga, Editor-in-Chief

Keywords: Rainfall Spatial variability Rainfall estimation Rain gauge network Debris flow

ABSTRACT

Rainfall in mountainous watershed presents high spatial variability due to elevation effects, and this introduces uncertainty in forecasting hydrological hazards such as water floods and debris flows. This study investigated the spatial variation of rainfall in a small watershed with a network of 10 rain gauges. A rainfall-elevation relationship was established based on data from 52 rainstorm events, which provides a method for rainfall estimation within the watershed. Result indicated that lower errors of interpolation occur when the rainfall amount is high, and that it is more difficult to estimate rainfall in high-elevation regions. Rain gauges become less representative when the distance between gauges is >3.0 km. The spatial variation of rainfall suggests that the gauge at the lowest elevation, or a single gauge within the source region, shows non-negligible errors with regard to calculating water flood discharge and identifying rainfall thresholds for debris flows. This study contributes to the understanding of event rainfall distribution and its impact on hydrological hazard forecasting in a small mountainous watershed.

1. Introduction

Rainfall is the most common inducing factor of hydrological hazards (e.g., water floods and debris flows) in mountainous watersheds with areas of $\leq\!50~\text{km}^2$ and large elevation differences (Wieczorek, 1996; Jakob et al., 2012; Hungr et al., 2014; Cui et al., 2018). Forecasting of such events is achievable through physical-based simulation (e.g., hydrological modeling) and/or empirical methods (e.g., statistical rainfall thresholds), both relying on rainfall as input. However, the rainfall data is highly uncertain due to measurement errors, systematic errors of interpolations, and intrinsic errors of rainfall randomness; these errors propagate through the model and directly impact the accuracy of forecasting. Therefore, a good knowledge of the uncertainty of rainfall data is essential for a correct forecasting of hydrological hazards.

Obtaining accurate rainfall data in mountainous region represents a major challenge (Krajewski et al., 2000, 2003). Radar and satellite remote sensing can provide nearly complete qualitative distributions of rainfall at high temporal and spatial resolutions, and both have become viable techniques for supplementing rainfall information (e.g., Fabry et al., 1994; Bradley et al., 2002; Kirschbaum et al., 2012; Rossi et al.,

2012; Marra et al., 2014; 2016). However, the coverage in many mountainous regions is poor. Thus, in most cases, ground-based rain gauge networks remain the only viable option for measurement of local rainfall (Habib et al., 2001). Unfortunately, the density of a rain gauge network is often too low to provide sufficient data. Therefore, estimations are often produced based on data recorded at neighboring gauges (e.g., Aleotti, 2004; Godt et al., 2006; Brunetti et al., 2010; Berti et al., 2012). In such cases, huge discrepancies can arise, the implications of which were clearly illustrated by the catastrophic debris flows in Zhouqu (China) on August 8, 2010, which caused 1765 fatalities. In the event, a gauge 16 km from the headwaters recorded 96 mm of rainfall, whereas the gauge at the outlet recorded only 3 mm (Hu et al., 2010; Cui et al., 2013). Such results exemplify the scale of the variation and uncertainty associated with rainfall in mountainous watersheds.

The spatial distribution of rainfall is complicated, and influenced by many orographic parameters (e.g., elevation, slope, aspect, shadowing, and curvature) and climatic factors (e.g., wind) (e.g., Goovaerts, 2000; Lloyd, 2005; Tobin et al., 2011), but it is hard to identify the major factors responsible for the high spatial variability of rainfall in small watershed (Dore et al., 1982). For a better understanding and

E-mail address: aaronguo@imde.ac.cn (G. Xiaojun).



^{*} Corresponding author at: Key Laboratory of Mountain Hazards and Surface Process/Institute of Mountain Hazards and Environment, Chinese Academy of Sciences, Chengdu 610041, China.

Journal of Hydrology 595 (2021) 126049

characterization, the local key influencing parameters should be considered. For instance, Spreen (1947) found that elevation alone explains 30% of the seasonal variance of rainfall while the combination of altitude, slope, exposure and orientation explained 88%. Basist et al. (1994) found slope gradient, orientation, elevation and exposure as the best mean annual precipitation predictors for 10 mountains. Strong winds may also redistribute the precipitation facilitating largest amounts in the valleys (Ye et al., 2004; Yang et al., 2005). Among the parameters, elevation can be considered as the most important because its influence remains constant, while that form others varies with events (Hevesi et al., 1992a; 1992b;; Goovaerts, 2000; Tobin et al., 2011). In most cases, on a given slope, rainfall typically increases with elevation, which is commonly called the orographic effect (e.g. Hutchinson, 1968; Vuglinski 1972; Hibbert, 1977; Smith 1979; Kumari et al., 2017); and generally, local rainfall increases with elevation in linear form, which has proved an acceptable approximation in many situations (e.g. Hibbert, 1977; Houghton, 1979; Obsorn, 1984; Buytaert et al., 2006). However, the characteristics of the relationship can vary appreciably from hillslope to hillslope. This make it difficult to obtain a usable relationship, unless rainfall stations are grouped into regions that control for such factors (Basist et al., 1994; Kumari et al., 2017). Although systematic uncertainties exist for measuring the rainfall amounts by gauges with regard to many factors, they can be reduced significantly by long-term and dense rainfall monitoring networks (Ye et al., 2004; Zhang et al., 2004; Xu et al., 2013; Ma et al., 2015; Kumari et al., 2017).

Objectives of rain gauge network design include effective rainfall measurement and determination of the effects of rainfall uncertainty to other hydrological variables (Bras et al., 1988). Gauge distribution significantly influences rainfall estimation. It has been suggested that only densely-distributed gauges are adequate for forecasting of rainfallinduced floods and debris flows (Haberlandt, 2007; Wagner et al., 2012). Interpolation based on geostatistical theory, which relies on a robust anisotropic variogram to define the spatial rainfall structure, is useful for rainfall estimation (e.g., Goovaerts, 1997; 2000; 2013; Price et al., 2000; Lloyd, 2005; Hancock and Hutchinson, 2006; Tobin et al., 2011; Wagner et al., 2012; Ly et al., 2011; Krivoruchko, 2012; Krivoruchko and Gribov, 2019). Unfortunately, the validation approach depends on the number and distribution of gauges, which are generally inadequate in data-sparse watersheds (Hattermann et al., 2005). Therefore, both the design of an effective monitoring network and choice of an interpolation method require insight into the variability and uncertainty of rainfall (Goovaerts, 2000; Buytaert et al., 2006). Several studies have proposed techniques to address the rainfall estimation uncertainty and its effects on hydrological hazard prediction (Jakob et al., 2012; Nikolopoulos et al., 2014, 2015). Most related studies have been conducted on long-term (i.e., monthly/daily) rainfall over large regions rather than on short-term rainfall events in small watersheds. The distinction is important because rainfall is more heterogeneous and pronounced over short timescales, and the degree of uncertainty is influenced primarily by the density of gauges (Nikolopoulos et al.,

In general, despite the complxity of mechanisms for spatial variation of rainfall, orographic variables are undoubtedly the tangible agencies; among which the elevation is the most conspicuous (Lloyd, 2005; Tobin et al., 2011). Therefore, in this study we analyzed the relationship between rainfall and elevation in a small mountainous watershed with large elevation difference, and proposed a rainfall estimation method. In addition, we assessed the estimation errors associated with elevation, rainfall amount, and gauge density using rainfall interpolation methods. Finally, the uncertainty of using different rainfall input data for forecasting floods and debris flows was evaluated to determine the effect of the representativeness of rain gauges.

2. Study area

Water floods and debris flows occur frequently and are widely

distributed throughout the basin of the Xiaojiang River, a tributary of the Jinsha River in Southwest China (Fig. 1). This semiarid mountainous area has high tectonic activity, abundant fragmented rocks, and large elevation differences. It is known for its poor ecological conditions and environmental disasters such as landslides, debris flows, soil erosion, and land debrisization. In addition to the geological and topographic conditions that are favorable for debris flow development, the mountains stimulate the occurrence of hydrological hazards by providing abundant rainfall and runoff for soil movement in headwater regions. Forecasting of the hazards is difficult because of the spatial variation of rainfall.

The Jiangjia Gully is located within the Xiaojiang River. It has an area of $48.6~\mathrm{km}^2$, and it extends from its drainage divide at an elevation of 3269 m to its outlet at 1042 m. It has been frequently impacted by tectonic activities (e.g., earthquakes) and has deeply cut sloping terrain over a large elevation range. This valley is known for frequent debris flow occurrences and long-term rainfall observations (Cui et al., 2005; Guo et al., 2013, 2016). Many studies have examined the mechanisms and triggering conditions of debris flows (e.g., Li et al., 2003, 2004, 2008; Cui et al., 2005, 2007). We selected it for this case study because of its dense rain gauge distribution (Fig. 1).

The valley can be divided into three climatic regimes. (1) A subtropical, dry, and hot valley climate extending from the outlet up to 1600 m, where the mean annual precipitation (MAP) is 600–700 mm, mean annual temperature (MAT) is 20 °C, and mean annual evaporation (MAE) is 3700 mm. (2) A subtropical, semiarid climate between 1600 and 2200 m, where MAP is 700–850 mm, MAT is 13 °C, and MAE is 1700 mm. (3) A humid climate above 2200 m, where MAP is 850–1200 mm, MAT is 7 °C, and MAE is 1350 mm. The variations in precipitation, temperature, and evaporation affect both vegetation distribution and rock weathering, and thus contribute in varying degrees to the occurrence of debris flows (Cui et al., 2015; Guo et al., 2020). To date, debris flows are mainly formed in the Menqian Gully, which is the northern branch (Fig. 1).

Ten rain gauges (R1–R10) have been installed in the watershed (Fig. 1). Based on monitoring data (2006–2017), the rainy season (May–September) accounts for approximately 85% of MAP. For example, at gauges R1 and R9, rainfall during the rainy season accounts for 83.0% and 89.7% of the total annual rainfall, respectively. The maximum daily rainfall amounts recorded at R1 and R9 are 53.5 and 63.1 mm, respectively, accounting for 9.4% and 10.0% of the total annual rainfall. Torrential rainstorms in summer are the main factor contributing to the frequent occurrence of debris flows.

3. Data source and methods

3.1. Data source

The length of the data records of the 10 rain gauges extends for more than a decade. The lowest-placed gauge (R1) is at the elevation of 1351 m in the downstream section (Fig. 1), whereas the others are all in the headwater regions at various elevations, as listed in Table 1. Each rain gauge measures real time rainfall using a 0.1-mm tipping bucket and the data are transmitted via the General Packet Radio Service. Rainfall events are separated with 6 h dry hiatuses (Restrepo-Posada and Eagleson, 1982). The rainfall amount of the event rainfall was therefore cumulated quantitatively from the beginning to the end of the rainfall. To identify the spatial characteristics of event rainfall within the watershed, we assessed the rainfall data recorded during 2006–2017 and selected 52 events in which the rainfall amount exceeded 10.0 mm at all gauges.

3.2. Methods

(1) Statistical methods

Two pairs of rain gauges were employed (R9 (2831 m) and R10

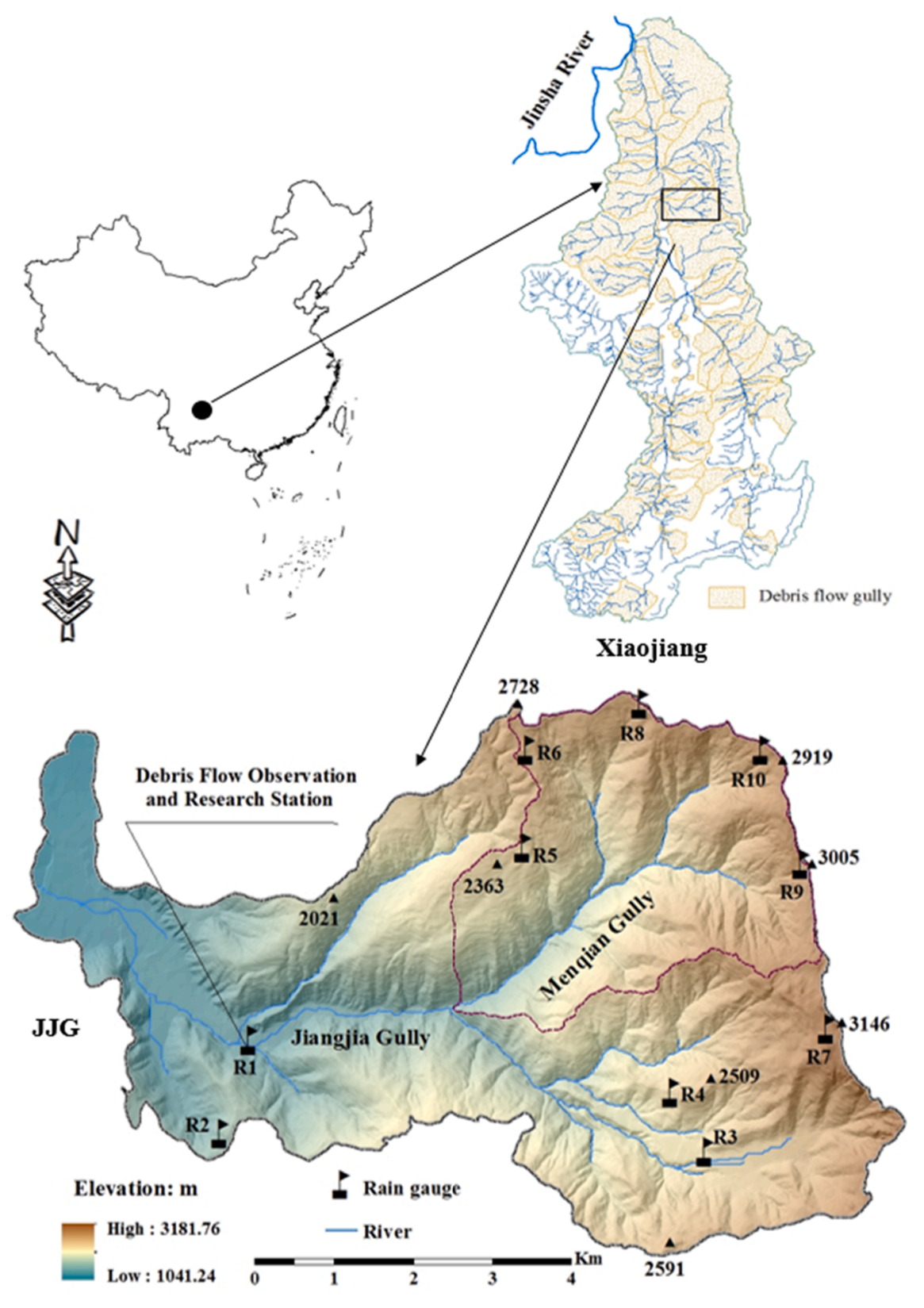


Fig. 1. Location, elevation, and rain gauge distribution of the Jiangjia Gully in Southwest China.

(2892 m), and R4 (2316 m) and R5 (2334 m)) to analyze the correlation and differences of rainfall data recorded at two gauges at similar elevation.

The Pearson correlation coefficient (Kendall and Stuart, 1963), a common statistical method, was used to reflect the level of similarity

between the 52 rainfall events. The Kolmogorov–Smirnov (K-S) normality test (Gauthier and Hawley, 2007), a special goodness-of-fit hypothesis test, was used to determine whether two datasets differed significantly. The K-S test has the advantage of making no assumption about the distribution of the data (i.e., it is nonparametric and

Table 1Elevation of rainfall gauges within the Jiangjia Gully watershed.

Date	R1	R2	R3	R4	R5	R6	R7	R8	R9	R10
Elevation (m)	1351	1636	2243	2316	2334	2592	2748	2818	2831	2892

distribution free).

(2) Rainfall interpolation

To investigate the uncertainty of gauge selection, we used three interpolation methods that included deterministic and probabilistic methods: inverse distance weighting (IDW), Empirical Bayesian Kriging (EBK), and Spline. Overall, the interpolated value of rainfall at a location is given by the weighted summation of known rainfall estimates (i.e., rain gauge data). Such geostatistical theories and methods are used widely used for rainfall interpolation (Lebel et al., 1987; Cressie, 1991; Goovaerts, 1997; 2000; Webster and Oliver, 2007; Bargaoui and Chebbi, 2009; Krivoruchko, 2012; Krivoruchko and Gribov, 2019).

(3) Rain gauge network configurations

We numerically generated rain gauge networks to investigate the effect of gauge densities and locations on interpolation results. Rain gauge networks were generated using tools in ArcGIS (ESRI, 2011). The geometric center of the watershed was set as the center of a square grid, having side lengths of l. Rain gauges were set at each grid intersection, with no consideration of topographic constraints on installation. Essentially, the real rainfall values from real gauges corresponding to the locations of the simulated gauge locations were used to mimic sampling of the rainfall field from a gauge network of the same density. The distance between two neighboring gauges were defined as l. In this case, the number of rain gauges (i.e., intersections) corresponded to sampling densities of l set to 0.5, 1, 1.5, 2, 2.5, 3, 3.5 and 4 km, respectively.

The gauge density as a key factor in analyzing rainfall estimation uncertainty was characterized by the distance between simulated gauges. Typically, the selection of mimic gauge locations relied on field experience, especially in low density cases. However, we found that rainfall interpolation results were similar for several configurations.

(4) Water flood and debris flow forecasting

A combination of the SCS-CN loss method for runoff yield and the kinematic wave method for slope and channel routing calculation was applied to evaluate the uncertainty of flood and debris flow forecasting (SCS, 1985; Mishra and Singh, 2003; Lumbroso and Gaume, 2012; Capra et al., 2018; Guo et al., 2020). The key parameters in the methods are the CN value and the slope and channel roughness coefficients: n_1 and n_2 , respectively. The parameters can be identified via lookup tables (SCS, 1985). In this work, the CN value for the watershed was set to 75, and coefficients n_1 and n_2 were set to 0.3 and 0.08, respectively; these values were held constant for each rainfall event and rainfall input scenario.

The intensity–duration (I-D) relationship for rainfall threshold is used for debris flow forecasting. Here, the duration (D) is defined as the period from the beginning of the rainfall event to onset of debris flow, and rainfall intensity (I) is considered as the mean intensity during period D (e.g., Caine, 1980; Guzzetti et al., 2007; 2008; Badoux et al., 2012; Berti et al., 2012).

4. Elevation influence on rainfall within the study area

Elevation, as mentioned above, is generally considered the most important topographic variable (Hevesi et al., 1992a; 1992b;; Goovaerts, 2000; Tobin et al., 2011). In the study area, although most of the gauges are located in headwater regions, the local landform is open flat ground. Therefore, as the effects of the other factors are difficult to quantify, the effect of elevation was primarily investigated.

4.1. Rainfall variation with elevation

The mean rainfall amount for each event was determined by averaging the values from all gauges. The values of each specific gauge were

also averaged for all events. These data showed that R1 had the lowest mean rainfall (18.4 mm), while R7 had the highest mean rainfall (31.9 mm)

Examination of these results also showed that rainfall varied markedly with elevation. In almost all cases, and for both mean and maximum values, rainfall increased with elevation (Fig. 2). The elevation of each gauge was normalized by dividing its elevation by that of R1 (1351 m) to avoid the exponent parameter becoming too small. Then the relationship between mean event rainfall values and normalized elevation appears as:

$$R_m = 8.9 e^{0.44h}, R^2 = 0.7902 (1)$$

where R_m is the mean event rainfall amount (mm) and h is the normalized elevation.

It was also found that the value of each rainfall was related to elevation, and that 39 of the 52 events (75%) present exponential relationships with $R^2 > 0.5$ (Fig. 3; based on 10 events). This suggests that Eq. 2 could be used to approximate the spatial variation of rainfall in most cases:

$$R = ae^{bh} (2)$$

where R is the rainfall amount (mm) and h is the normalized elevation; and coefficient a (range: 4.50–35.83) and exponent b (range: 0.255–0.857) define the rainfall variance.

4.2. Differences between gauges at similar elevations

We assessed the correlation between the rainfall measured at similar elevations using data from two pairs of gauges: R4 (2316 m) and R5 (2334 m), and R9 (2831 m) and R10 (2892 m). The horizontal distance between the gauge pairs was 4.1 (R4–R5) and 1.8 km (R9–R10). The expectation (E) and standard deviation (σ) of the rainfalls are listed in Table 2. The Pearson correlation coefficient (P) was used to evaluate the similarity of the rainfall for each pair. At a significance level of 0.01, P was 0.857 and 0.789, respectively for R4–R5 and R9–R10, indicating high similarity. Event rainfall for each pair is presented on 1:1 scatterplots in Fig. 4a and 4b. The average deviation was 18.8% and 7.5%, respectively, indicating a certain degree of variance.

The results of the K-S normality test, which was used to analyze the difference between the two data series, indicated no significant

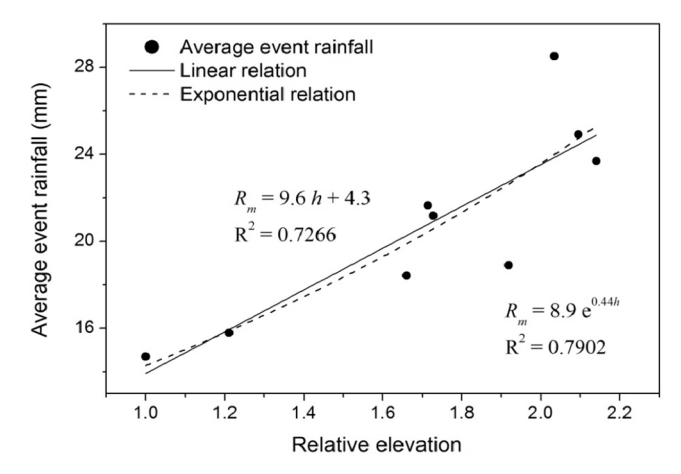


Fig. 2. Relationship between mean rainfall and elevation in the study area.

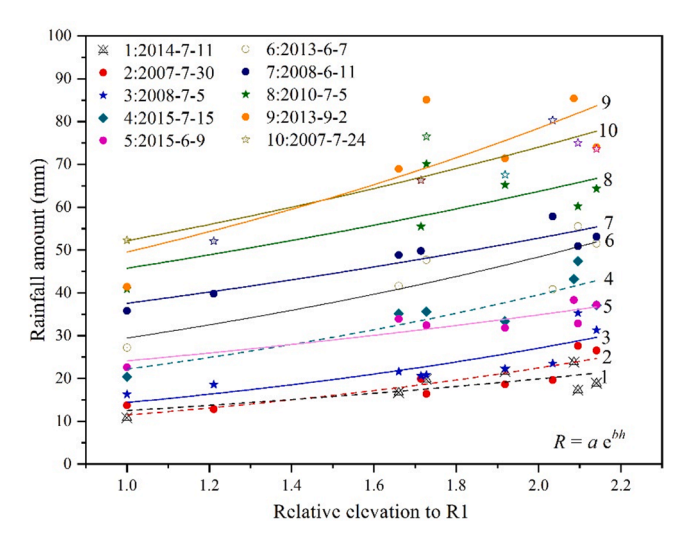


Fig. 3. Data showing the exponential relationship between rainfall amount and gauge elevation.

Table 2 Expectation and standard deviation values for the 52 rainfall events at selected gauges.

Rain gauge	E	σ	n	P
R9	40.9	14.1	49	0.857
R10	41.9	15.1	50	
R4	37.1	14.9	27	0.789
R5	40.6	18.0	46	

n is the number of rain events recorded.

difference. The high correlation and non-significant difference between the mean rainfall amounts for the two gauge sets, where each component shared the same elevation with its pair, indicate that evident effect of the elevation to the rainfall variation.

4.3. Rainfall estimation based on elevation

The rainfall value at a specific location can be calculated by weighted summation of rainfall records. However, such interpolation relies on a dense network of rain gauges, which is typically unavailable in mountainous regions. If strong correlation exists between rainfall and topographic variables, then the variables could be used for rainfall

estimation (Lloyd, 2005; Tobin et al., 2011).

Recorded data indicat that the coefficient a is linearly related to the minimum rainfall (i.e., R_1 , as represented by record at R1), and exponent b reflects the increase in rainfall with elevation (Fig. 5):

$$a = mR_1 - n \tag{3}$$

$$b = clna + d \tag{4}$$

where m,n,c, and d are constant coefficients . In this study, the values of the coefficients were set as $c=1.53,\,d=0.32,\,m=0.69,$ and n=1.04.

Combining Eqs. 2, 3, and 4, the relationship between rainfall amount and gauge elevation can be expressed as

$$R = e^{ch} (mR_1 - n)^{ch+1} R_1^{-dh} = (0.69R_1 - -1.04) R_1^{-0.32h} e^{1.53h}$$
 (5)

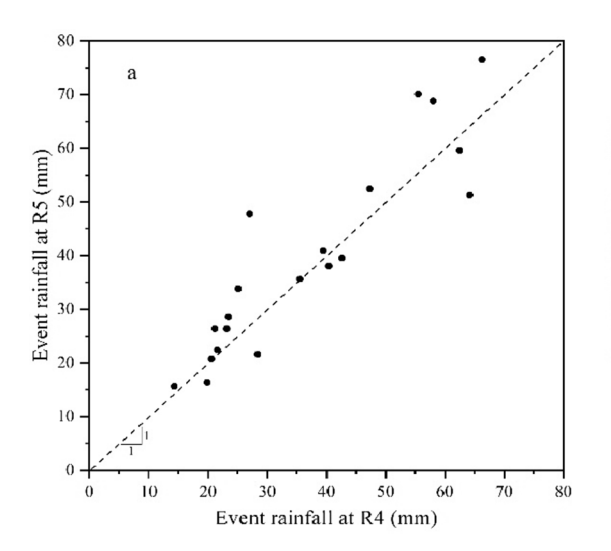
where R is the rainfall at a specified location in the watershed (mm), R_1 is the rainfall collected at rain gauge R1 (mm), and h is the elevation relative to R1. Using Eq. 5, the rainfall value at each point within the watershed was calculated based on the R1 value for each rainfall event. The errors associated with this method are shown in Fig. 6.

In Fig. 6, the error of the EBK method is used as the *x*-axis, and it can be seen that the error of both the IDW and the Spline methods is close to that of the EBK method. The average errors of the IDW, EBK, and Spline methods are 2.0%, 1.1%, and 1.5% at R4, respectively, and 8.5%, 7.5%, and 8.6% at R6, respectively. In most cases (22 of 26 events at R4 and 37 of 45 events at R6), the value calculated using Eq. 5 was an overestimation compared with the recorded rainfall amount. The errors of 7.9% and 17.8% at R4 and R6, respectively, are much larger than those of traditional interpolation methods. This is expected and acceptable because this estimation depends on a single gauge (i.e., the lowest gauge, which is generally located at the watershed outlet) rather than on a dense rain gauge network.

Approximately, the higher the rainfall value at R1, the lower the absolute error values at both R4 and R6 (Fig. 7). If an error of 40% were acceptable for rainfall estimations at both R4 and R6, then the rainfall recorded at R1 should be > 15.0 and > 17.5 mm, respectively. Given that R6 has a longer record than R4, a 17.5-mm rainfall threshold is adopted as the condition on R1 for Eq. 5. It ensures that the higher the rainfall amount, the stronger the relationship between rainfall and elevation, and thus the better the estimations.

5. Uncertainties of rainfall interpolation and effects of gauge distance

Density and location of ground-based rain gauges are crucial factors



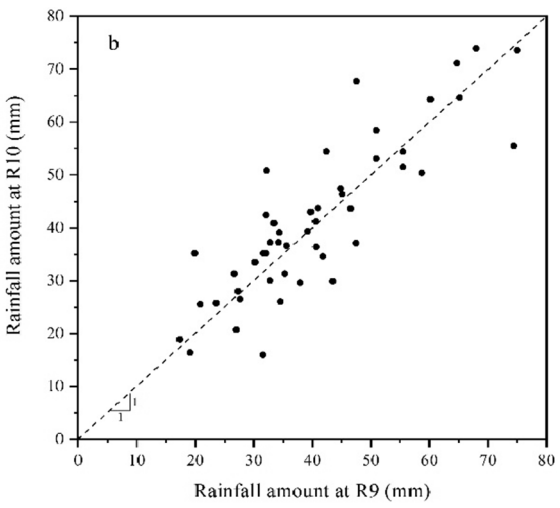
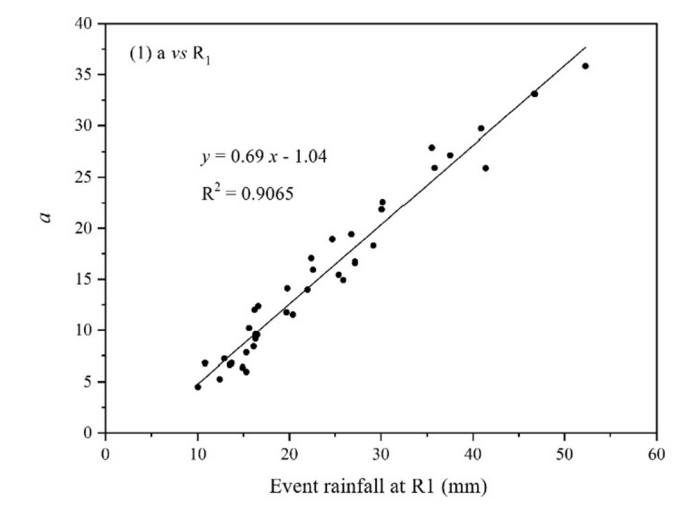


Fig. 4. Comparison of event rainfall amounts recorded at similar elevations: (a) R4-R5 and (b) R9-R10.



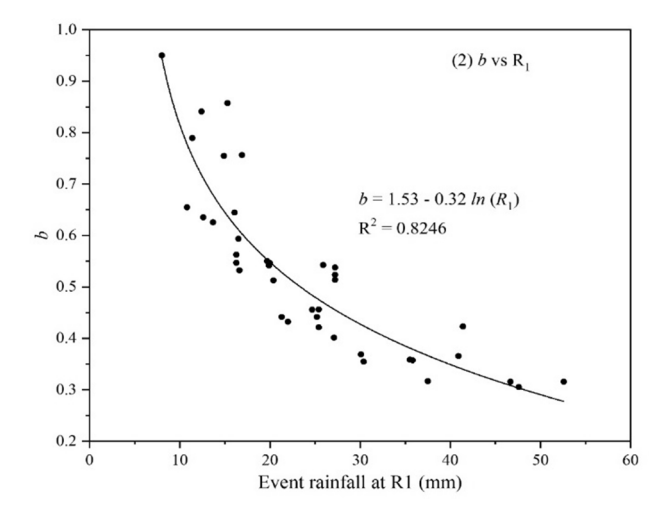


Fig. 5. Relationship between rainfall amount at R1 and (a) coefficient a and (b) exponent b.

that require careful consideration, as they significantly affect the accuracy of rainfall-induced hazard parameter calculations (Duncan et al., 1993). The distance between gauges, which reflects the representative range of each gauge, requires careful evaluation (Bradley et al., 2002; Villarini et al., 2008, 2014).

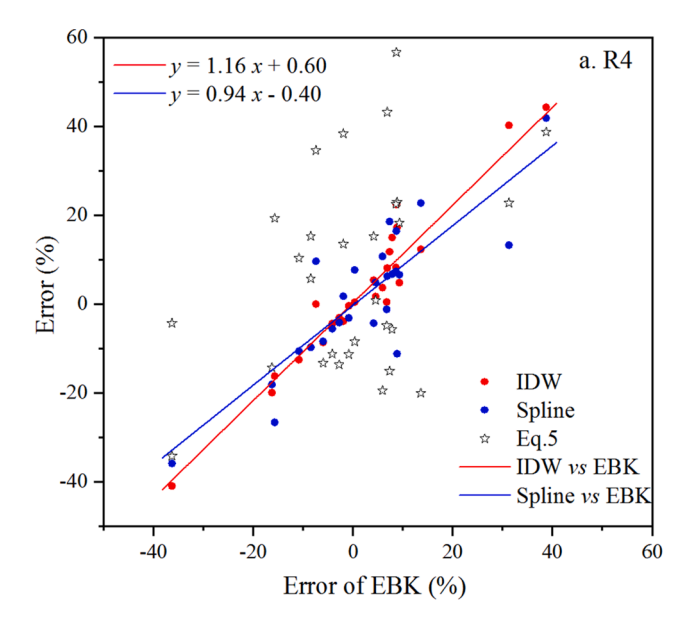
5.1. Rain gauge network configurations

We numerically generated rain gauge networks to investigate the effect of gauge density and location on the interpolation results. The distance (*I*) between two gauges was set separately as 0.5, 1.0, 1.5, 2.0, 2.5, 3.0, 3.5, and 4.0 km, which represent different gauge densities and numbers, as shown in Fig. 8.

Rainfall values were assigned to each gauge based on the rainfall distribution within the watershed. Therefore, for each rainfall event, we used Eq. 5 to calculate the rainfall amount at each simulated gauge and at the watershed center point (CC). Subsequently, rainfall was interpolated over the entire watershed using the IDW, EBK, and Spline methods. Interpolation results for each real gauge were compared with background values calculated using Eq. 5, which provided reference values for the analysis.

5.2. Uncertainty of rainfall interpolation

Progressively denser rain gauge networks are belived to produce



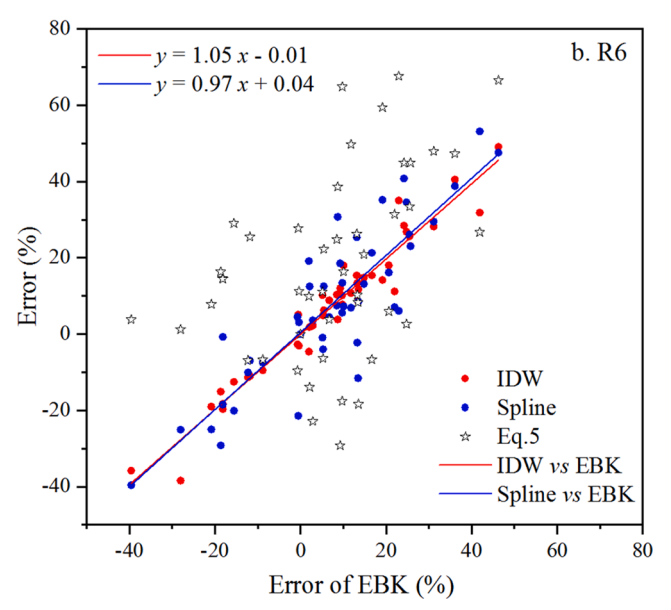
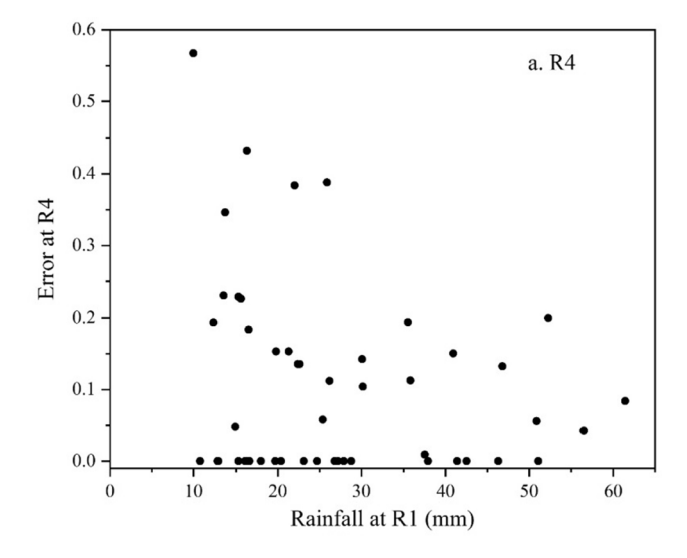


Fig. 6. Errors of inverse distance weighting (IDW), Spline, and Eq. 5 vs. the error of Empirical Bayesian Kriging (EBK).

increasingly accurate rainfall interpolation results. In this case, the interpolation errors were presented with a gauge separation distance of 0.5 km, i.e., the densest configuration. The results for four gauges (R1, CC, R4, and R10 at elevation of 1351, 1838, 2316, and 2892 m, respectively) are shown in Fig. 9, based on which the following observations can be made.

- (1) The absolute error of any of the three methods was no higher than 6%, suggesting high accuracy, as if the data used for the interpolation were abundant.
- (2) The error property (positive or negative) for each interpolation method was the same for each gauge. In general, the mean error was negative, indicating that rainfall was underestimated by all interpolation methods and in all rain gauge density scenarios, except at R1. This also indicates that on average rainfall was overestimated by Eq. 5.
- (3) Lower errors of interpolation occurred when rainfall amounts were high. This pattern was consistent for all interpolation



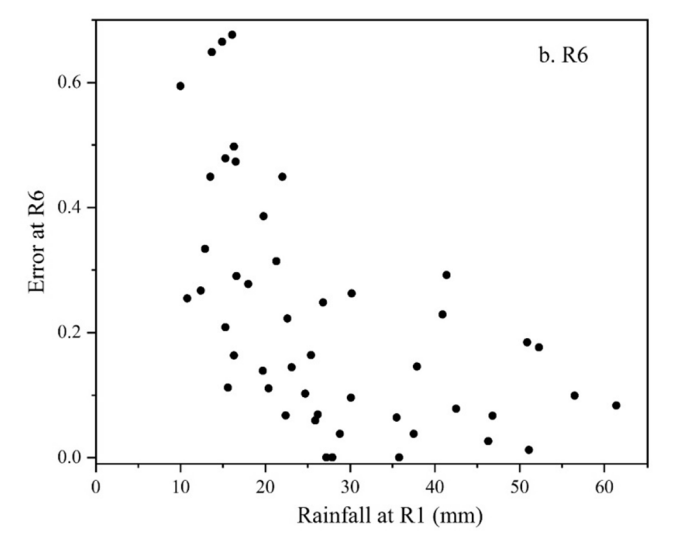


Fig. 7. Data showing the relationship between rainfall estimation errors at two gauges: (a) R4 and (b) R6, based on Eq. 5 and rainfall amount at R1.

methods, although the error rate varied among the different methods.

The relationship between estimation error and gauge elevation was investigated under each gauge configuration. As the IDW, EBK, and Spline methods showed similar tendency with elevation, only the results obtained using IDW are discussed here. All errors were arithmetically averaged by the absolute values of the real errors, and they are shown by the black line in Fig. 10.

Error values were small at low elevations and the mean error increased with elevation. Over the elevation range 1300-1900~m (R1, R2, and CC), errors were 1.4%-10.2% with average of 4.9%-6.3%. Over the elevation range 2000-2400~m (R3–R5), errors were 2.7%-10.8% with average of 6.1%-9.2%. Errors increased to 3.7%-19.4% (average: 10.4%-15.6%) over elevation range 2600-2900~m at the headwater region of the watershed (R6–R10). These results imply that it is more difficult to estimate rainfall in high-elevation regions.

5.3. Effective distance for rain gauges

Rain gauge density might cause significant bias in estimation of rainfall thresholds for debris flows (Nikolopoulos et al., 2014). Although the interpolation errors were different for all three studied methods,

their tendencies were similar. As such, the results obtained using the IDW method are used to illustrate the effect of gauge density on interpolation error.

Inclusion of more rain gauges within a network might be expected to produce more accurate interpolation results (Nikolopoulos et al., 2014); however, this was not the case in this study. Instead, the interpolation errors reflected the variation of gauge configuration. It can be seen that the error lines associated with each rainfall event are parallel (Fig. 11, taking R1 and R2 as examples). The maximum and minimum errors for each rainfall event for all 10 rain gauges are shown in Fig. 12. In most cases, the errors changed smoothly over gauge distances of 0.5-2.5 km but changed abruptly for distances of 2.5-3.0 km. This is apparent in the error data for the average watershed rainfall shown in Fig. 13. Although the errors decreased as the grid length increased over the 0.5-2.5-km range, the error variations are very small (-1% to -5%). In contrast, the errors increased abruptly at the 3.0-km grid length, leading to less reliable results. These findings suggest that rain gauge placement should be considered carefully when the horizontal distance between gauges in a network is >3.0 km.

6. Effect of uncertainties of gauge selection on hydrological hazard forecasting

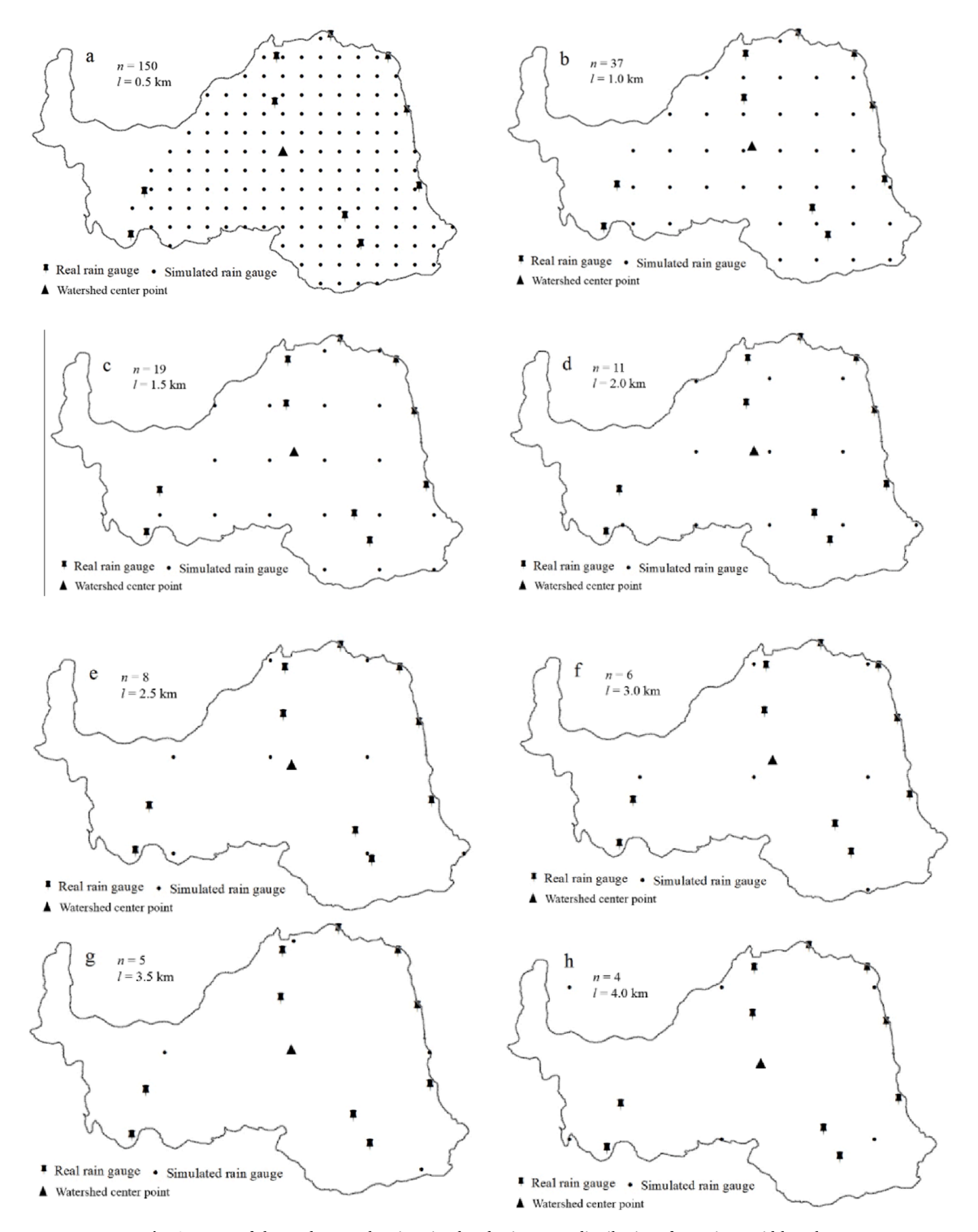
The quality of rainfall data significantly affects the accuracy of hydrological modeling and hazard forecasting, but dense gauge network is impractical in most mountainous regions. At best, in most circumstances, the arrangement consists of one gauge at the outlet, or inside the watershed if there is an established local village. This deficiency presents a serious challenge because data from one gauge might not be sufficiently representative of the watershed, especially in regions with high spatial variation in the distribution of rainfall. Thus, the following section discusses the uncertainties caused by the selection of different gauges, from the perspectives of water flood discharge simulation and the determination of rainfall thresholds for debris flow forecasting.

6.1. Influence of gauge selection on hydrological simulation

In the study region, water floods are doubly problematic, because in addition to causing their own catastrophic damage, they are also responsible for triggering debris flows. We selected eight rainfall events to investigate the influence of rain gauge selection on peak discharge and total water quantity measurements by setting up different inputs for hydrological simulations. These eight events represented a range of varying rainfall amounts and durations.

Four rainfall input scenarios were designed that consisted of interpolation based on the following: I) all 10 rain gauges, II) one of the rain gauges in the high-elevation headwater region (R9), III) the lowest station in the Jiangjia Gully main channel (R1), and IV) rainfall calculated using Eq. 5. Among them, scenario I is regarded as the most accurate input; thus, results from the other scenarios were compared with this scenario. A combination of the SCS-CN loss method for runoff yield and the kinematic wave method for slope and channel routing calculation was applied. The *CN* value for the watershed was set to 75, and this was held constant for each rainfall event and rainfall input scenario. The simulation results are shown in Figs. 14 and 15.

Results for scenario III (using R1 at the lowest elevation to represent rainfall conditions throughout the entire watershed) show that the water flood was seriously underestimated in all cases, with non-referential results. In contrast, the results for scenario II (using R9 in the headwater region) show that the water flood was overestimated in most cases (7 in 8 cases). This not only demonstrates that rainfall increases with elevation but also highlights the uncertainties caused by inappropriate rain gauge selection. However, when using the estimation of Eq. 5 as the rainfall input (scenario IV), the errors were much smaller. The peak discharge simulation errors were in the range of [-14.0%, 23.5%], while the errors of the total water flood amount are in the range of



 $\textbf{Fig. 8.} \ \ \text{Maps of the study area showing simulated rain gauge distributions for various grid lengths}.$

[-11.8%, 16.4%]. These results exhibit acceptable accuracy, especially considering the difficulty of obtaining rainfall data in mountainous areas.

6.2. Effect of uncertainties of gauge selection on rainfall thresholds for debris flows

The *I-D* relationship is a common approach for identification of rainfall thresholds in debris flow forecasting (e.g., Caine, 1980; Guzzetti et al., 2007; 2008). The determination of rainfall thresholds is often

performed based on long-term historical rainfall data. To estimate the magnitude of the errors in threshold identification caused by the rainfall estimation, we used the 52 rainfall events, 19 of which triggered debris flows

The rainfall was selected from the following: (1) the most representative gauge, which was determined based on detailed analysis of the rainfall and the monitoring of the debris flow processes. As debris flow initiation in the source regions was not monitored, when a debris flow appeared at the monitoring section, the rainfall process was investigated based on gauges located in the source regions. In particular,

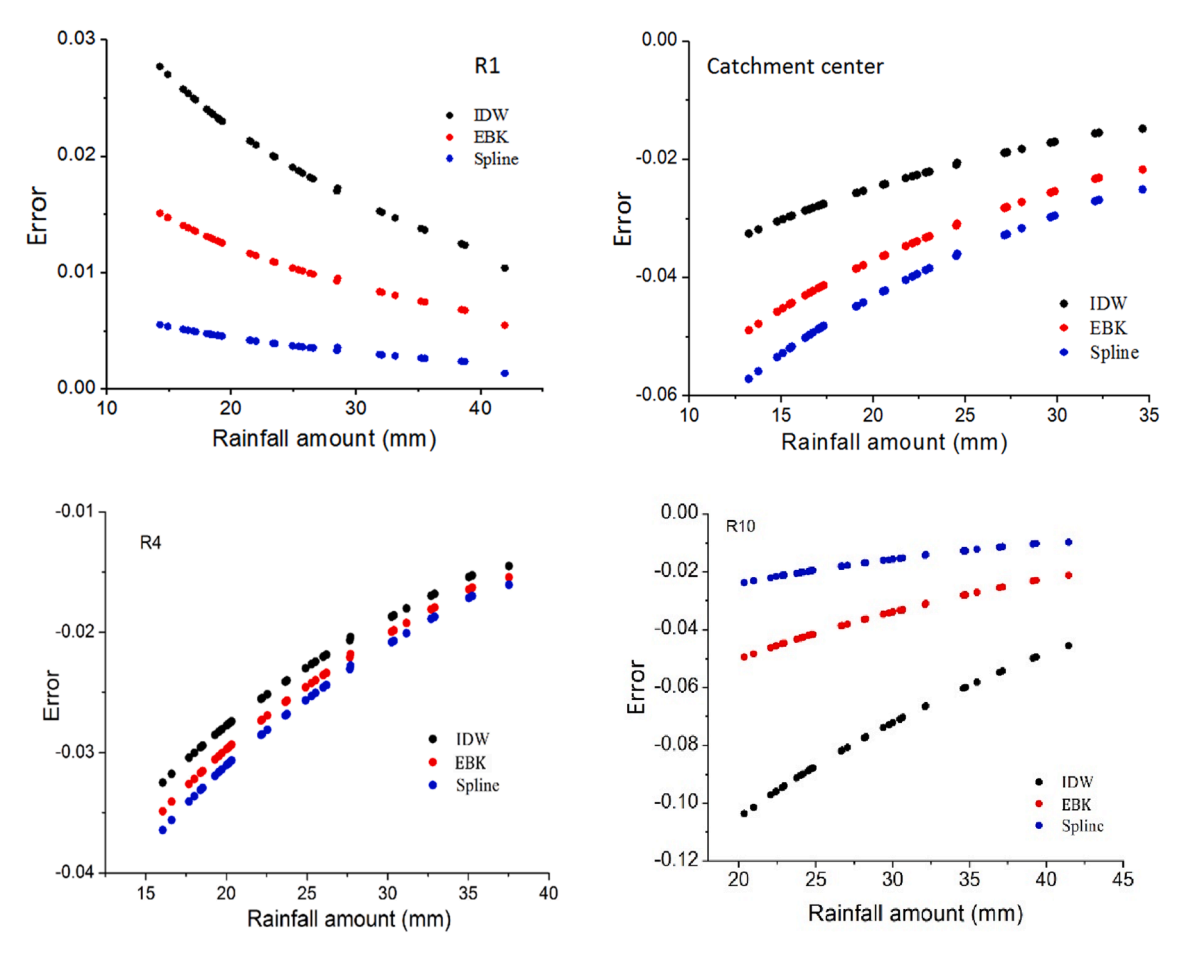


Fig. 9. Relative rainfall estimation errors for R1, CC, R4, and R10 based on the three interpolation methods.

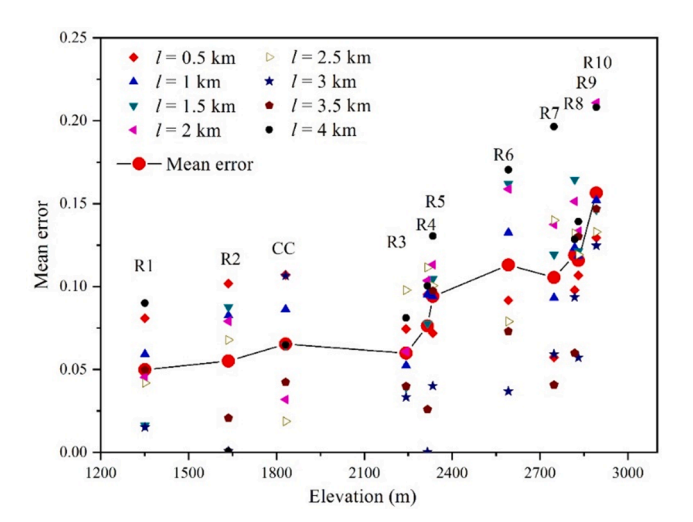


Fig. 10. Inverse distance weighting interpolation errors in rainfall estimation with increasing elevation.

consideration was given to both the time lag between debris flow appearance and peak rainfall, and the differences in the rainfall process between the gauges (Guo et al., 2020); (2) R1, located at the mouth of the watershed; (3) R7, at elevation in the source areas, about 5 km from the catchment center (Fig. 1); and (4) the rainfall estimated using Eq. 5. This examination considers both the influence of elevation and gauge distance. In essence, the rainfall thresholds were compared with the actual *I-D* threshold to evaluate the effectiveness of using rainfall data

from different sources.

The threshold was identified as $I=11.23\ D^{-0.710}$ by selecting the most representative gauge. The false alarm and false negative rates, defined as percentages of the total numbers, were 34% and 0%, respectively, and the results obtained for the other three scenarios were compared with these results. It has been suggested that debris flows in this watershed are most likely triggered during rainfall events with duration of < 16.8 h (Fig. 16). Therefore, considering the traditional duration used in forecasting by the China Meteorological Department, rainfall durations of 1, 12, and 24 h were assumed and the 1-h, 12-h, and 24-h rainfall amounts required to trigger debris flows were estimated. The results are shown in Fig. 17.

When using R1 as the rainfall information source, the threshold was identified as $I=8.28\,D^{-0.751}$, with false alarm and false negative rates of 47% and 0%, respectively, and the required 1-, 12-, and 24-h rainfall amounts were evidently underestimated. When using the rainfall from R7, the threshold was $I=15.81\,D^{-0.748}$, the false alarm and false negative rates were 24% and 32%, respectively, and the error of the 1-h rainfall amount was overestimated by as much as 40.8%. However, for the rainfall calculated using Eq. 5, the rainfall threshold was identified as $I=12.98\,D^{-0.707}$, which is closer to the real threshold, and the false alarm and false negative rates were 30% and 11%, respectively. In addition, the error evaluation results were substantially lower than for the other two scenarios (Fig. 17).

The results indicate that the rain gauge should be selected carefully when identifying the rainfall conditions in the source region responsible for initiation of debris flows. The rain gauge at the watershed outlet, which is commonly used in mountainous regions, generally underestimates the rainfall condition. In addition, representativeness should also be considered when using an alternative gauge within the

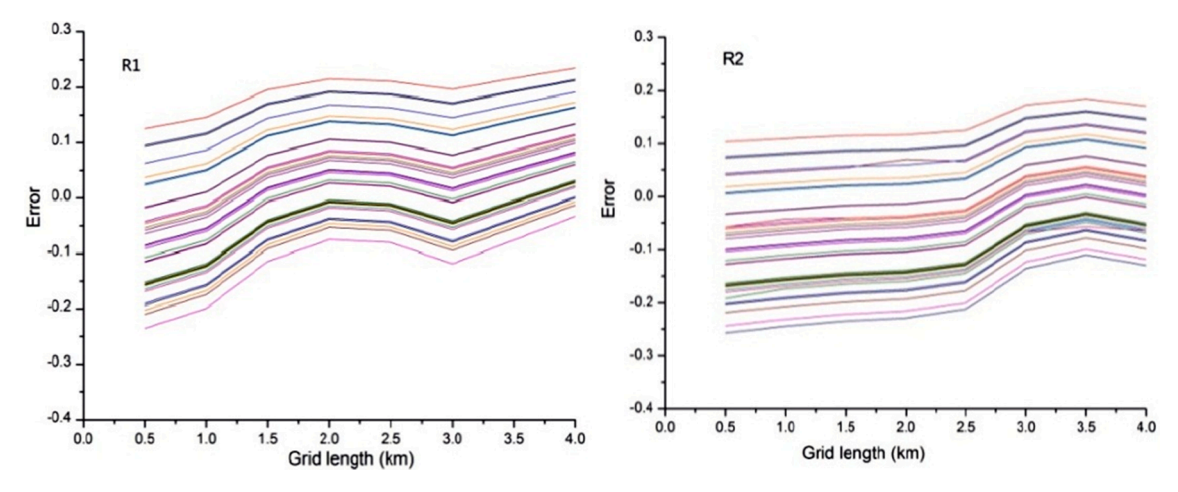


Fig. 11. Rainfall estimation errors of the inverse distance weighting interpolation method for different grid lengths at R1 and R2.

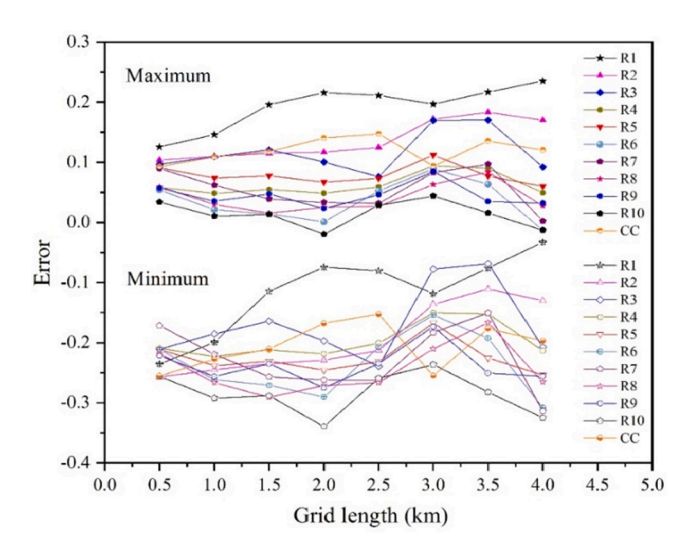


Fig. 12. Maximum and minimum errors for different grid lengths at each gauge.

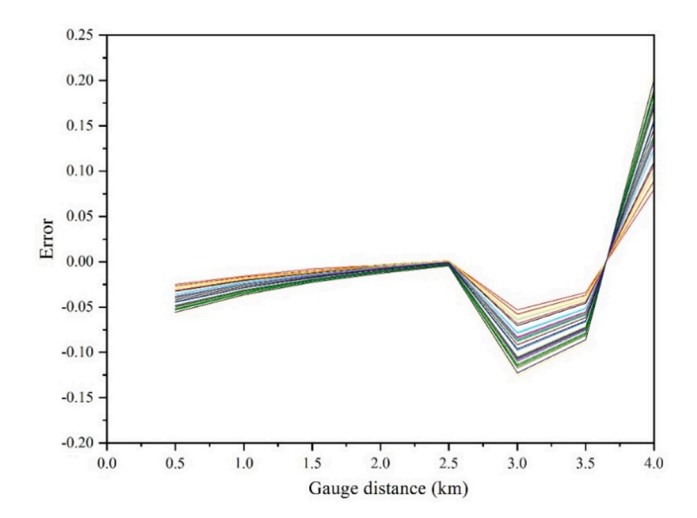


Fig. 13. Errors of average watershed rainfall based on the inverse distance weighting interpolation method for gauge networks with different grid lengths.

watershed but with a distance of > 3 km from the debris flow source region. In contrast, the better performance achieved using Eq. 5 indicates that the spatial variation of rainfall cannot be neglected, and that the relationship between rainfall and elevation could be used for estimating rainfall within a watershed.

7. Discussion

As rainfall is a crucial factor for hydrological hazards, many advanced approaches (e.g., radar and satellite remote sensing) have been developed in recent years for rainfall estimation. Radar quantitative precipitation estimation is an active and vibrant field with numerous accomplishments resulting in practical applications (e.g., Germann et al., 2006; Yoshikawa et al., 2012; Chen et al., 2017; Shimamura et al., 2016; Chandrasekar et al., 2018). It is expected to improve our knowledge of rainfall processes by providing greater dynamic range, more detailed information on microphysics, and better accuracies in rainfall estimation. This information will not only give us insight into microphysical processes but also provide detailed properties of the rainfall (Chandrasekar et al., 2008). With the local bias correction of the ground gauge data, it has been used for hydrological hazards forecasting recently (Peleg et al., 2013; Mei et al., 2014; Espinosa et al., 2015; Zhang et al., 2016; Willie et al., 2017; Shi et al., 2018). Yet, even with the success, more complete coverage is needed, both spatially and temporally, especially for a small mountainous catchment and an event rainfall scale. In regions such as the study area, gauge measurements remain the most effective means for data collection. Some recent studies have proposed that ground-based measurements of rainfall are to some extent not sufficiently reliable for interpolation purposes; however, this largely reflects the insufficient quantity of gauges (e.g., Frei and Schar, 1998; Goovaerts, 2000; Lloyd, 2005; Ly et al., 2011; Tobin et al., 2011; Marra et al., 2014; 2016; Thakur et al., 2020).

In the previous research, it has been found that rainfall increases with elevation, which commonly called the orographic enhancement, typically approximate a linear form in most cases, is evident (Hibbert, 1977; Houghton, 1979; Obsorn, 1984; Daly et al., 1994; Sanchez-Moreno et al., 2013). The focuses are the average amount or the accumulated amount of long-term period (e.g. annual and month rainfall). In this study, although a general exponential increasing tendency of rainfall with elevation was proposed, the linear tendency of the average rainfall of 52 events is also evident (Fig. 2), which indicated consistent with the findings of other related research (e.g., Vuglinski, 1972; Hibbert, 1977; Smith, 1979; Kumari et al., 2017; Hevesi et al., 1992a; 1992b;; Goovaerts, 2000).

The analysis used measurements from 10 rain gauges in a small watershed, which represented a dense gauge network and a reliable data

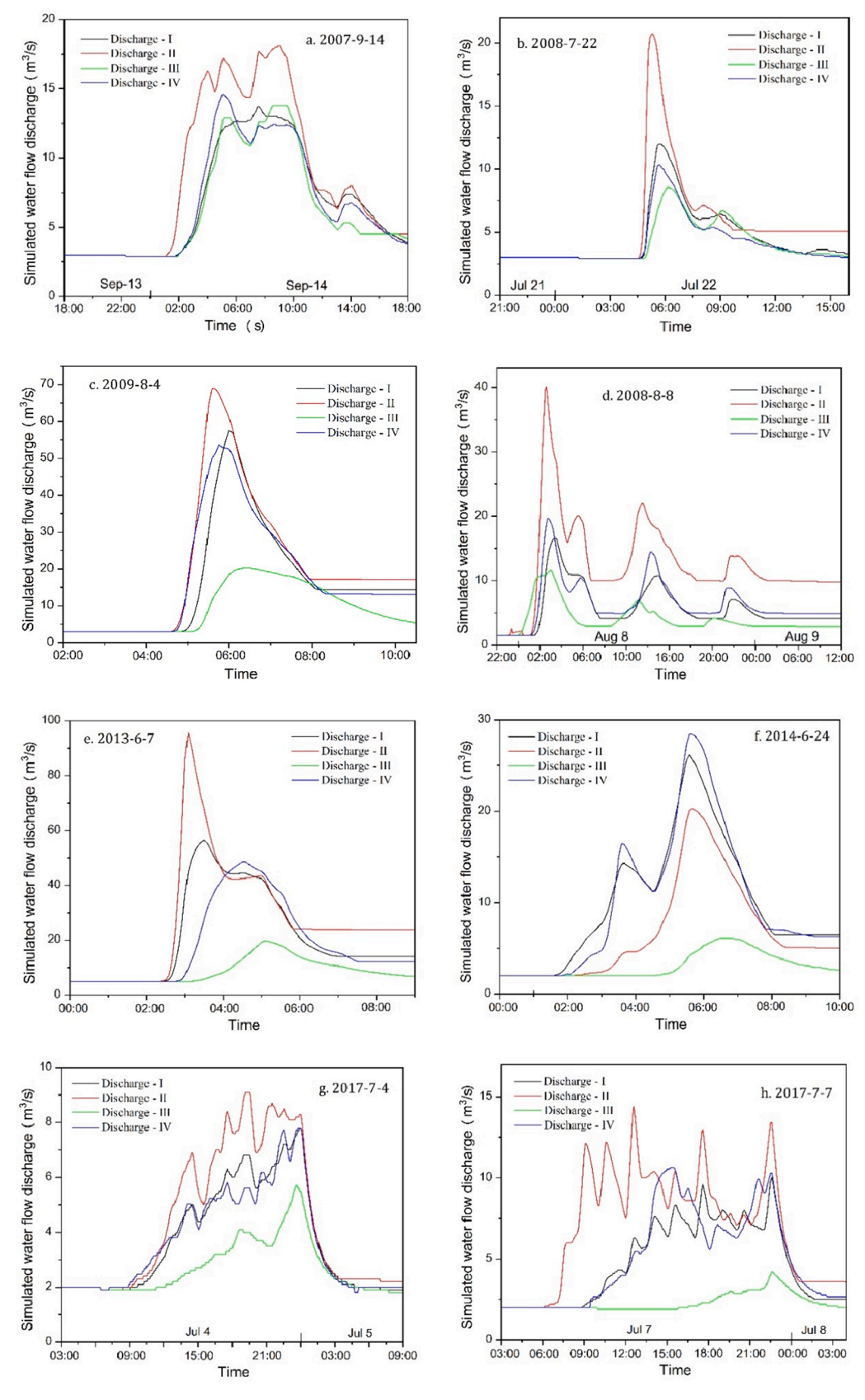


Fig. 14. Hydrological simulation results of water floods in eight rainfall events with four rainfall input scenarios.

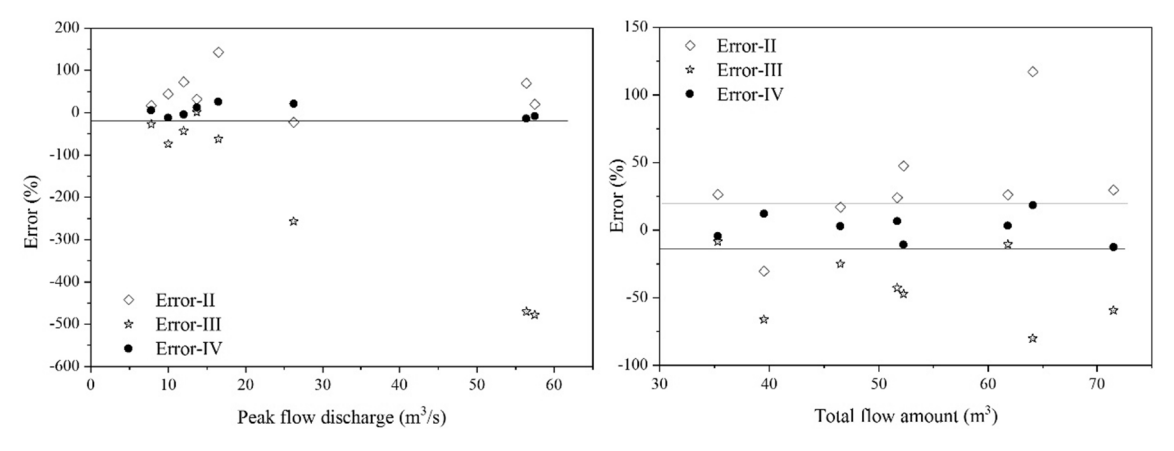


Fig. 15. Errors of peak flow discharge and total flow amount for each scenario.

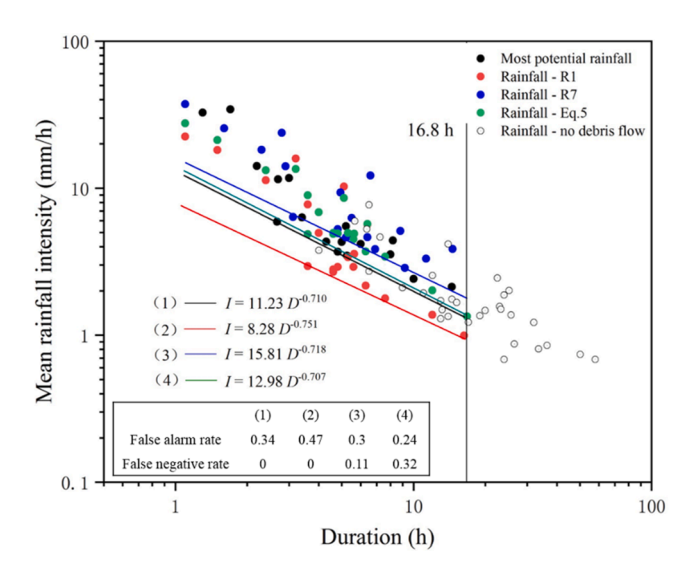


Fig. 16. *I-D* rainfall thresholds determined using rainfall from different gauges and calculated using Eq. 5.

source. Here, we assume that the measured natural rainfall is the real rainfall without data correction. Although it is well known that rainfall amounts measured by means of ground gauges contain some negative biases, the evaluation of such uncertainty is not the purpose of this work. The findings of this study could provide a reference for rainfall

estimation in neighboring regions with similar climatic and topographic conditions, and help improve the understanding of debris flow formation conditions and forecasting. However, the feasibility of using a similar network in other debris flow regions is not guaranteed owing to potential regional differences.

8. Conclusions

Spatial variation of rainfall is a phenomenon that introduces large uncertainty in the forecasting of hydrological hazards (e.g., water floods and debris flows). This is particularly so for small mountainous watersheds with complex orographic conditions. In this study, 52 rainstorm events in a typical small mountainous watershed were used to analyze the relationships between event rainfall and both the elevation and the density of rain gauges.

The high correlation and consistent similarity in rainfall amounts between gauges at similar elevation suggested that elevation is the primary factor affecting rainfall variation in this region. Results showed that the mean event rainfall and elevation exhibited an exponential relationship. Moreover, rainfall amount varied with elevation in each event. Thus, an empirical rainfall–elevation relation was proposed for rainfall estimation. Although the accuracy of this method was poorer than that of commonly used interpolation methods, it is advantageous in that it requires only the rainfall data recorded at the watershed outlet.

In addition, the rainfall interpolation uncertainties and effects of gauge distance were evaluated. All interpolation results showed a similar error tendency and demonstrated that estimating rainfall distributions at high elevations is more difficult. Error analysis indicated

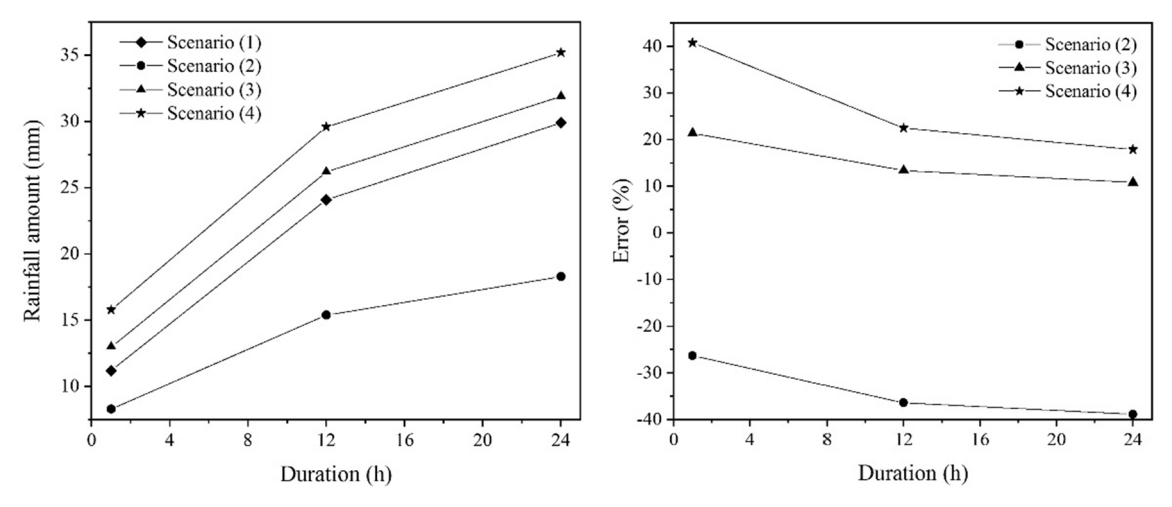


Fig. 17. The 1-, 12-, and 24-h rainfall amounts required to trigger debris flows, and the errors associated with each approach.

that rain gauges should be placed carefully when the horizontal distance between gauges is $> 3.0 \ \mathrm{km}$.

Selecting an inappropriate rain gauge for obtaining data caused significant uncertainty in simulations of water flood discharge and in identification of rainfall thresholds for debris flows. Using a gauge located at the mouth of the watershed, or in the headwater region, produced poorer performance in terms of flow simulation and empirical threshold identification for debris flows, when compared with the estimation method proposed in this work. This suggests that the representativeness of the rain gauge should be considered carefully, and that clear understanding of the spatial variation of rainfall could help in estimation of the rainfall conditions required for initiation of hydrological hazards.

Declaration of Competing Interest

The authors declare that they have no known competing financial interests or personal relationships that could have appeared to influence the work reported in this paper.

Acknowledgments

This study was supported by the National Research and Development Program of China (2020YFD1100701 and 2017YFC1502504), NSFC (41977257), the Strategy project of CAS (XDA23090202) and Western Light of Young Scholars, CAS. We thank the Dongchuan Debris Flow Observation and Research Station for the rainfall data. We are also grateful to James Buxton MSc from Liwen Bianji, Edanz Group China (www.liwenbianji.cn/ac), for editing the English text of this manuscript.

References

- Aleotti, P., 2004. A warning system for rainfall-induced shallow failures. Eng. Geol. 73, 247–265.
- Badoux, A., Turowski, J.M., Mao, L., Mathys, N., Rickenmann, D., 2012. Rainfall intensity-duration thresholds for bedload transport initiation in small Alpine watersheds. Nat. Hazards Earth Syst. Sci. 12 (10), 3091–3108.
- Bargaoui, Z.K., Chebbi, A., 2009. Comparison of two kriging interpolation methods applied to spatiotemporal rainfall. J. Hydrol. 365, 56–73.
- Basist, A., Bell, G.D., Meentemeyer, V., 1994. Statistical relationships between topography and precipitation patterns. J. Clim. 7, 1305–1315.
- Berti, M., Martina, M.L.V., Franceschini, S., Pignone, S., Simoni, A., Pizziolo, M., 2012.
 Probabilistic rainfall thresholds for landslide occurrence using a Bayesian approach.
 J. Geophys. Res. 117, F04006.
- Bradley, A.A., Peters-Lidard, C., Nelson, B.R., Smith, J.A., Young, C.B., 2002. Raingauge network design using NEXRAD precipitation estimate. JAWRA J. Am. Water Resour. Assoc. 38, 1393–1407.
- Bras, R.L., Tarboton, D.G., Puente, C., 1988. Hydrologic sampling: a characterization in terms of rainfall and basin properties. J. Hydrol. 102 (1–4), 113–135.
- Brunetti, M.T., Rossi, M., Luciani, S., Valigi, D., Guzzetti, F., 2010. Rainfall thresholds for the possible occurrence of landslides in Italy. Nat. Hazards Earth Syst. Sci. 10, 447–458.
- Buytaert, W., Celleri, R., Willems, P., Bièvre, B.D., Wyseure, G., 2006. Spatial and temporal rainfall variability in mountainous areas: a case study from the south Ecuadorian Andes. J. Hydrol. 329, 413–421.
- Caine, N., 1980. The rainfall intensity-duration control of shallow landslides and debris flows. Geografiska Annaler. Series A. Phys. Geogr. 62, 23–27.
- Capra, L., Coviello, V., Borselli, L., Márquez-Ramírez, V.-H., Arámbula-Mendoza, R., 2018. Hydrological control of large hurricane-induced lahars: evidences from rainfall, seismic and video monitoring. Nat. Hazards Earth Syst. Sci. 18, 781–794.
- Chandrasekar, V., Hou, A., Bringi, V.N., Rutledge, S.A., Gorrucci, E., Peterson, W., Jackson, G., 2008. Potential role of Dual-Polarization Radar in the validation of satellite precipitation measurements: rationale and opportunities. Bull. Am. Meteorol. Soc. 89, 1127–1145.
- Chandrasekar, V., Chen, H., Philips, B., 2018. Principles of high-resolution radar network for hazard mitigation and disaster management in an urban environment. J. Meteorol. Soc. Jpn. 96A.
- Chen, H., Chandrasekar, V., Bechini, R., 2017. An improved dual-polarization radar rainfall algorithm (DROPS2.0): application in NASA IFloodS field campaign. J. Hydrometeorol. 18, 917–937.
- Cressie, N.A., 1991. Statistics for Spatial Data. John Willey & Sons, New York.
- Cui, P., Chen, X.P., Wang, Y.Y., Hu, K.H., Li, Y., 2005. Jiangjia Ravine debris flows in the southwestern China. In: Jakob, M., Hungr, O. (Eds.), Debris-flow Hazards and Related Phenomena. Springer-Verlag, pp. 565–594.
- Cui, P., Guo, X.J., Yan, Y., Li, Y., Ge, Y.G., 2018. Real-time observation of an active debris flow watershed in the Wenchuan Earthquake area. Geomorphology 321, 153–166.

- Cui, P., Zhou, G.D., Zhu, X.H., Zhang, J.Q., 2013. Scale amplification of natural debris flows caused by cascading landslide dam failures. Geomorphology 182, 173–189.
- Cui, P., Zhu, Y.Y., Chen, J., Han, Y.S., Liu, H.J., 2007. Relationships between antecedent rainfall and debris flows in Jiangjia Ravine, China. In: Chen, C.L., Major, J.J. (Eds.), Debris-flow Hazard Mitigation-Mechanics, Prediction, and Assessment. Millpress, Rotterdam, pp. 1–10.
- Daly, C., Neilson, R.P., Phillips, D.L., 1994. A statistical-topographic model for mapping climatological precipitation over mountainous terrain. J. Appl. Meteorol. 33 (2), 140–158
- Dore, A.J., Choularton, T.W., Brown, R., Blackall, R.M., 1982. Orographic enhancement in the mountains of the Lake District and Snowdonia. Atmos. Environ. 26A, 357–371
- Duncan, M.R., Austin, B., Fabry, F., Austin, G.L., 1993. The effect of gauge sampling density on the accuracy of streamflow prediction for rural watersheds. J. Hydrol. 142, 445–476.
- ESRI. ArcMap Version 10 User Manual. ESRI: Redlands, CA, USA, 2011.
- Espinosa, B., Hromadka II, T.V., Perez, R., 2015. Comparison of radar data versus rainfall data. MethodsX 2, 423–431.
- Fabry, F., Bellon, A., Duncan, M.R., Austin, G.L., 1994. High resolution rainfall measurements by radar for very small basins: the sampling problem reexamined. J. Hydrol. 161, 415–428.
- Frei, C., Schar, C., 1998. A precipitation climatology of the Alps from high-resolution rain-gauge observations. Int. J. Climatol. 18, 873–900.
- Gauthier, T.D., Hawley, M.E., 2007. Statistical methods. Introduction to Environmental Forensics, Second ed.
- Germann, U., Galli, G., Boscacci, M., Bolliger, M., 2006. Radar precipitation measurement in a mountainous region. Q. J. Roy. Meteor. Soc. 132, 1669–1692.
- Godt, J.W., Baum, R.L., Chleborad, A.F., 2006. Rainfall characteristics for shallow landsliding in Seattle, Washington, USA. Earth Surf. Process. Landf. 31, 97–110.
- Goovaerts, P., 1997. Geostatistics for Natural Resources Evaluation. Oxford Univ. Press, New York.
- Goovaerts, P., 2000. Geostatistical approaches for incorporating elevation into the spatial interpolation of rainfall. J. Hydrol. 228, 113–129.
- Guo, X.J., Cui, P., Li, Y., 2013. Debris flow warning threshold based on antecedent rainfall: a case study in Jiangjia Ravine, Yunnan, China. J. Mount. Sci. 10 (2), 305–314.
- Guo, X.J., Li, Y., Cui, P., 2016. Discontinuous slope failures and pore-water pressure variation. J. Mount. Sci. 13 (1), 116–125.
- Guo, X.J., Li, Y., Cui, P., Yan, H., Zhuang, J.Q., 2020. Intermittent viscous debris flow formation in Jiangjia Gully from the perspectives of hydrological processes and material supply. J. Hydrol. (under review).
- Guzzetti, F., Peruccacci, S., Rossi, M., Stark, C., 2007. Rainfall thresholds for the initiation of landslides in central and southern Europe. Meteorol. Atmos. Phys. 98, 239–2125.
- Guzzetti, F., Peruccacci, S., Rossi, M., Stark, C., 2008. The rainfall intensity–duration control of shallow landslides and debris flows: an update. Landslides 5, 3–17.
- Haberlandt, U., 2007. Geostatistical interpolation of hourly precipitation from rain gauges and radar for a large-scale extreme rainfall event. J. Hydrol. 332, 144–157.
- Habib, E., Krajewski, W.F., Kruger, A., 2001. Sampling errors of fine resolution tipping-bucket rain gauge measurements. J. Hydrol. Eng. 6 (2), 159–166.
- Hancock, P.A., Hutchinson, M.F., 2006. Spatial interpolation of large climate data sets using bivariate thin plate smoothing splines. Environ. Modell. Software 21, 1684–1694.
- Hattermann, F., Krysanova, V., Wechsung, F., Wattenbach, M., 2005. Runoff simulations on the macroscale with the ecohydrological model SWIM in the Elbe catchmentvalidation and uncertainty analysis. Hydrol. Process. 19, 693–714.
- Hevesi, F., Istok, J., Flint, A., 1992a. Precipitation estimation in mountainous terrain using multivariate geostatistics. Part I: structural analysis. J. Appl. Meteor. 31, 661–676.
- Hevesi, F., Flint, A., Istok, J., 1992b. Precipitation estimation in mountainous terrain using multivariate geostatistics. Part I: Isohyetal maps. J. Appl. Meteor. 31, 677–688.
- Hibbert, A., 1977. Distribution of precipitation on rugged terrain in central Arizona. Hydrol. Water Resour. Ariz, Southwest 7, 163–173.
- Houghton, J., 1979. A model for orographic precipitation in north-central Great Basin. Mon. Wea. Rev. 107, 1462–1475.
- Hu, K.H., Ge, Y.G., Cui, P., Guo, X.J., Yang, W., 2010. Preliminary Analysis of Extralarge-scale debris flow disaster in Zhouqu County of Gansu province. J. Mount. Sci. 28 (5), 628–634 (in Chinese).
- Hungr, O., Leroueil, S., Picarelli, L., 2014. The Varnes classification of landslide types, an update. Landslides 11, 167–194.
- Hutchinson, P., 1968. An analysis of the effect of topography on rainfall in Taieri Catchment area. Otago. Earth Sci. J. 2, 51–68.
- Jakob, M., Owen, T., Simpson, T., 2012. A regional real-time debris-flow warning system for the District of North Vancouver, Canada. Landslides 9, 165–178.
- Kendall, M.G., Stuart, A., 1963. The Advanced Theory of Statistics: Distribution Theory. Hafner, New York, pp. 60–62.
- Kirschbaum, D.B., Adler, R., Hong, Y., Kumar, S., Peters-Lidard, C., Lerner-Lam, A., 2012. Advances in landslide nowcasting: evaluation of a global and regional modeling approach. Environ. Earth Sci. 66, 1683–1696.
- Krajewski, W.F., Ciach, G.J., Habib, E., 2003. An analysis of smallscale rainfall variability in different climatic regimes. Hydrol. Sci. J. 48, 151–162.
- Krajewski, W.F., Ciach, G.J., McCollum, J.R., Bacotiou, C., 2000. Initial validation of the global precipitation climatology project monthly rainfall over the United States. J. Appl. Meteorol. 39, 1071–1087.
- Krivoruchko, K., 2012. Empirical Bayesian Kriging. ArcUser Fall 2012.

- Krivoruchko, K., Gribov, A., 2019. Evaluation of empirical Bayesian kriging. Spat. Stat. 32 https://doi.org/10.1016/j.spasta.2019.100368.
- Kumari, M., Singh, C., Bakimchandra, O., Basistha, A., 2017. Geographically weighted regression based quantification of rainfall-topography relationship and rainfall gradient in Central Himalayas. Int. J. Climatol. 37, 1299–1309.
- Lebel, T., Bastin, G., Obled, C., Creutin, J., 1987. On the accuracy of areal rainfall estimation—a case-study. Water Resour. Res. 23, 2123–2134.
- Li, Y., Hu, K.H., Yue, Z.Q., Tham, T.G., 2004. Termination and deposition of debris-flow surge. In: Landslides: Evaluation and Stabilization. Taylor & Francis Group, London, pp. 1451–1456.
- Li, Y., Kang, Z.C., Yue, Z.Q., Tham, L.G., Lee, C.F., Law, K.T., 2003. Surge waves of debris flow in Jiangjia Gully, Kunming. China. In: Fast Slope Movements Prediction and Prevention for Risk Mitigation, pp. 303–307.
- Li, Y., Su, P.C., Cui, P., Hu, K.H., 2008. A probabilistic view of debris flow. Journal of Mountain Science. 5 (2), 91–97.
- Lloyd, C.D., 2005. Assessing the effect of integrating elevation data into the estimation of monthly precipitation in Great Britain. J. Hydrol. 308, 128–150.
- Ly, S., Charles, C., Degré, A., 2011. Geostatistical interpolation of daily rainfall at watershed scale: the use of several variogram models in the Ourthe and Ambleve watersheds. Belgium. Hydrol. Earth Syst. Sci. 15, 2259–2274.
- Ly, S., Charles, C., Degré, A., 2013. Different methods for spatial interpolation of rainfall data for operational hydrology and hydrological modeling at watershed scale. A review. Biotechnol. Agron. Soc. Environ. 17, 392–406.
- Lumbroso, D., Gaume, Eric, 2012. Reducing the uncertainty in indirect estimates of extreme flash flood discharges. J. Hydrol. 414–415, 16–30.
- Mishra, S.K., Singh, V.P., 2003. Soil conservation service curve number (SCS-CN) Methodology. Kluwer Academic Publishers, Dordrecht, The Netherland, p. 2003.
- Ma, Y., Zhang, Y., Yang, D., Farhan, S.B., 2015. Precipitation bias variability versus various gauges under different climatic conditions over the Third Pole Environment (TPE) region. Int. J. Climatol. 35, 1201–1211.
- Marra, F., Nikolopoulos, E.I., Creutin, J.D., Borga, M., 2014. Radar rainfall estimation for the identification of debris-flow occurrence thresholds. J. Hydrol. 519 (Part B), 1607–1619.
- Marra, F., Nikolopoulos, E.I., Creutin, J.D., Borga, M., 2016. Space–time organization of debris flows-triggering rainfall and its effect on the identification of the rainfall threshold relationship. J. Hydrol. 541 (Part A), 246–255.
- Mei, Y., Anagnostou, E.N., Nikolopoulos, E.I., Borga, M., 2014. Error analysis of satellite precipitation products in mountainous basins. J. Hydrometeorol. 15, 1778–1793.
- Nikolopoulos, E.I., Crema, S., Marchi, L., Marra, F., Guzzetti, F., Borga, M., 2014. Impact of uncertainty in rainfall estimation on the identification of rainfall thresholds for debris flow occurrence. Geomorphology 221, 286–297.
- Nikolopoulos, E.I., Marra, F., Creutin, J.D., Borga, M., 2015. Estimation of debris flow triggering rainfall: influence of rain gauge density and interpolation methods. Geomorphology 243, 40–50.
- Obsorn, H., 1984. Estimating precipitation in mountainous regions. J. Hydraul. Eng. 110, 1859–1863.
- Peleg, N., Ben-Asher, M., Morin, E., 2013. Radar subpixel-scale rainfall variability and uncertainty: lessons learned from observations of a dense rain-gauge network. Hydrol. Earth Syst. Sci. 17, 2195–2208.
- Price, D.T., McKenney, D.W., Nalder, I.A., Hutchinson, M.F., Kesteven, J.L., 2000. A comparison of two statistical methods for spatial interpolation of Canadian monthly mean climate data. Agric. For. Meteorol. 101, 81–94.
- Restrepo-Posada, P.J., Eagleson, P.S., 1982. Identification of independent rainstorms. J. Hydrol. 55 (1–4), 303–319.
- Rossi, M., Kirschbaum, D., Luciani, S., Mondini, A.C., Guzzetti, F., 2012. TRMM satellite rainfall estimates for landslide early warning in Italy: preliminary results.

- Proceedings of SPIE The International Society for Optical Engineering. 8523, art. no. 85230D.
- Sanchez-Moreno, J.F., Mannaerts, C.M., Jetten, V., 2013. Influence of topography on rainfall variability in Santiago Island. Cape Verde. Int. J. Climatol. 34 (4), 1081–1097.
- Shi, Z., Wei, F.Q., Chandrasekar, Venkatachalam, 2018. Radar-based quantitative precipitation estimation for the identification of debris flow occurrence over earthquake-affected regions in Sichuan. China. Nat. Hazards Earth Syst. Sci. 18, 765–780.
- Shimamura, S., Chandrasekar, V., Ushio, T., et al., 2016. Probabilistic attenuation correction in a networked radar environment. IEEE Trans. Geosci. Remote Sens. 54 (12), 6930–6939.
- Smith, R., 1979. The influence of mountains on the atmosphere. Advances in Geophysics, Academic Press. 21: 87-230.
- SCS., 1985. Hydrology. National Engineering Handbook, Soil Conservation Service. USDA, Washington, DC.
- Spreen, W.C., 1947. Determination of the effect of topography upon precipitation. Transactions of the American Geophysical Union 28 (2), 285–290.
- Thakur, M.K., Desamsetti, S., Rajesh, A. N., Koteswara, K.R., Narayanan, M.S., Kumar. T. V. L., 2020. Exploring the rainfall data from satellites to monitor rainfall induced landslides A case study. Advances in Space Research. Doi: 16/j.asr.2020.05.015.
- Tobin, C., Nicotina, L., Parlange, M.B., Berne, A., Rinaldo, A., 2011. Improved interpolation of meteorological forcings for hydrologic applications in a Swiss Alpine region. J. Hydrol. 401, 77–89.
- Villarini, G., Mandapaka, P.V., Krajewski, W.F., Moore, R.J., 2008. Rainfall and sampling uncertainties: a rain gauge perspective. J. Geophys. Res. 113, D11102.
- Villarini, G., Seo, B.C., Serinaldi, F., Krajewski, W.F., 2014. Spatial and temporal modeling of radar rainfall uncertainties. Atmos. Res. 135–136, 91–101.
- Vuglinski, V., 1972. Methods for the study of laws for the distribution of precipation in medium-high mountains (illustrated by the Vitim River basin). Distribution of Precipatation in Mountainous Areas, WMO Pub. 326 (2), Geneva, 212-221.
- Wagner, P.D., Fiener, P., Wilken, F., Kumar, S., Schneider, K., 2012. Comparison and evaluation of spatial interpolation schemes for daily rainfall in data scarce regions. J. Hydrol. 464, 388–400.
- Webster, R., Oliver, M.A., 2007. Geostatistics for environmental scientists. John Wiley & Sons Ltd, Chichester, UK.
- Wieczorek, G.F., 1996. Landslide triggering mechanisms. Landslides: investigation and mitigation. pp: 76–90.
- Willie, D., et al., 2017. Evaluation of multi sensor quantitative precipitation estimation in Russian River Basin. J. Hydrol. Eng. 22 (5), E5016002. (ASCE) HE.1943-5584.0001422.
- Xu, H., Xu, C.-Y., Chen, H., Zhang, Z., Li, L., 2013. Assessing the influence of rain gauge density and distribution on hydrological model performance in a humid region of China. J. Hydrol. 505 (15), 1–12.
- Yang, D., Kane, D., Zhang, Z., Legates, D., Goodison, B., 2005. Bias-corrections of long-term (1973–2004) daily precipitation data over the northern regions. Geophys. Res. Lett. 32. L19501.
- Ye, B., Yang, D., Ding, Y., Han, T., Koike, T., 2004. A bias-corrected precipitation climatology for China. J. Hydrometeorol. 5, 1147–1160.
- Yoshikawa, E., Ushio, T., Kawasaki, Z., Chandrasekar, V., 2012. Dual-directional radar observation for preliminary assessment of the Ku-band broadband radar network. J. Atmos. Ocean. Technol. 29, 1757–1768.
- Zhang, Y., Ohata, T., Yang, D., Davaa, G., 2004. Bias correction of daily precipitation measurements for Mongolia. Hydrol. Process. 18, 2991–3005.
- Zhang, J., Howard, K., Langston, C., et al., 2016. Multi-Radar Multi-Sensor (MRMS) quantitative precipitation estimation: initial operating capabilities. Bull. Am. Meteorol. Soc. 97, 621–626.